Hindawi Publishing Corporation
International Journal of Rotating Machinery
Volume 2016, Article ID 8628467, 16 pages
http://dx.doi.org/10.1155/2016/8628467

Research Article

Flow Pattern Analysis and Performance Improvement of Regenerative Flow Pump Using Blade Geometry Modification

J. Nejadrajabali, A. Riasi, and S. A. Nourbakhsh

Department of Mechanical Engineering, University of Tehran, P.O. Box 115554563, Tehran 14174 66191, Iran

Correspondence should be addressed to A. Riasi; ariasi@ut.ac.ir

Received 24 December 2015; Revised 24 January 2016; Accepted 26 January 2016

Academic Editor: Tariq Iqbal

Regenerative pump is a low specific speed and rotor-dynamic turbomachine capable of developing high heads at low flow rates. In this paper, a numerical study has been carried out in order to investigate the effect of blade angle on the performance of a regenerative pump. Two groups of impellers were employed. The first type has symmetric angle blades with identical inlet/outlet angles of ±10°, ±30°, and ±50° and the second group has nonsymmetric angle blades in which the inlet angle was set to 0° and six different angles of ±10°, ±30°, and ±50° were designed for the outlet of the blades. A total of 12 impellers, as well as primary radial blades impeller, were investigated in this study. The results showed that all forward blades have higher head coefficients than radial blades impeller at design flow coefficient. It was found that regenerative pumps with symmetric angle forward blades have better performance than other types. Also, it is worth mentioning that the highest head coefficient and efficiency occur at angle $+10 < \beta < +30$ of symmetric angle blades. It was found that the maximum efficiency occurs at angle of +15.5° by curve fitting to the data obtained from numerical simulations for symmetric angle forward blades.

1. Introduction

Regenerative flow pumps are placed in the category of dynamic pumps. The ability to produce high heads at low flow rates is the main characteristic of these pumps. The specific speed of regenerative pumps is very low and they share some of the characteristics of positive displacement pumps without any wear and lubrication problems. The fluid in regenerative pump moves spirally in flow channel and reenters the blades of impeller several times in its peripheral path from inlet to outlet. Because of this repetitive treatment of impeller blading on fluid, regenerative pumps have the ability to generate a head equivalent to that of several centrifugal stages with comparable tip speeds. The regenerative pumps are less likely to cause cavitation, because of its smaller pressure gradient, than centrifugal pumps. Therefore, regenerative pumps, typically, require lower net positive suction head than centrifugal pumps [1]. Typically, regenerative pumps have a disadvantage of having a low hydraulic efficiency (between 30 and 50%).

Regenerative pumps have found applications in many industrial areas which require high heads at low flow rates including automotive and aerospace fuel pumping, booster systems, water supply, agricultural industries, shipping and mining, and chemical and food processing systems [2].

In 1955, Wilson et al. offered a mathematical analysis for regenerative pumps with radial blades that have already been used. They considered helical flow and made various allowances for losses and provided experimental corroborations of their results. The calculated and experimental performance curves were compared and excellent agreement was observed [3]. Song et al. modified Wilson's theory. They introduced loss models in a manner that does not require empirical coefficients and experimental results. But their analysis was just accurate at design point [4]. Yoo et al. in 2005 presented equations to calculate the geometry of rotating flows. They attempted to develop an improved mathematical model to suggest systematic methods to find the circulatory flow rate, mean inlet and outlet radii of the impeller, and slip factor [1]. Based on this improved momentum exchange theory, they studied the design of a regenerative flow pump for artificial heart pump application [5]. These models require experimental support to determine a number of empirical coefficients in the proposed models. In particular these models do not take account of the influence of blade angle on the

performance, and hence they have limited applicability as a design tool [6].

There are few articles that studied the effect of geometric variables of the regenerative pumps. Shimosaka and Yamazaki studied the changes in the number of blades, clearance and channel area in a regenerative pump. In the experiments the flow channel was fixed and in each test, change in one parameter was examined. They introduced a parameter named "characteristic dimension of flow channel" to define the limit value for clearance and channel area. Another parameter called "width ratio of vane" was applied to determine number of blades [7]. Yamazaki and Tomita studied regenerative pumps with nonradial blades with different side channel areas. They proposed some correlation coefficients and empirical equations for efficiency, torque, and head coefficient as functions of Reynolds number, blade angle, side channel area, and flow coefficient [8–10]. Grabow studied the effects of the blade angle for both radial and semicircular blades. He tested the pump in both cases with different blade angles in the range of ±60°. He found from the theoretical study that the optimum shut-off head was reached for the blade angle in the range of 40°–55°, but the experimental results showed the optimal blade angle in the range of 40°–45° [11]. Sixsmith and Altmann studied the regenerative compressor with airfoil blades. They added a core in the flow channel to direct the circulating flow together with the provision of airfoil blades. It resulted in significant improvements in the performance. They found that the airfoil blades produced more pressure rise than any other blade shapes [12]. Badami investigated the effect of clearances, number of blades, blade angles, and channel area on the performance of regenerative pumps. He presented a new model of regenerative pump with axial inlet and outlet port [13]. Choi et al. carried out an experimental study to investigate the influence of blade angle on the performance of regenerative pump. The influence of the impeller blade angle and its shape on regenerative pump performance has been experimentally investigated. Straight blades with inclined blade angles of 0°, ±15°, ±30°, and ±45° were tested. In addition radial chevron impellers with chevron angles of 15°, 30°, and 45° were also included in their experiments. It was found that the head and the efficiency strongly depend on the blade angles as well as the blade geometry. Among all blade configurations tested in this study, the chevron blade exhibited the highest head with reasonably good efficiency. The results showed that there was an optimum chevron angle of around 30° [6].

In recent years, computational fluid dynamics (CFD) has been widely used for the analysis of fluid flow in turbomachinery. But the number of articles in the field of numerical methods for the study of flow in the regenerative turbomachines is very low.

Meakhail et al. in 2003 used CFX software to study the swirling flow in a regenerative pump with radial blades. They found that, in addition to the tip of blades, the flow exits from the side edge [14]. Teshome and Dribsa used a commercial code to investigate the effect of aerodynamic blades on the performance of regenerative pump. They extracted the performance curves for pump from CFD simulations. They found out that significant improvement of performance has been obtained in using aerodynamic blades with semielliptic profile [2]. Quail et al. used FLUENT software to investigate the fluid flow in a regenerative pump. The results of CFD simulations were validated by the experimental data. They also used a novel method of manufacturing to evaluate the effect of change in blade geometry on the efficiency of pump [15, 16]. Vasudeva Karanth et al. used CFD analysis in order to enhance the performance of regenerative pump. It was seen as a significant effect on the pump performance by varying the number of blades and changing the geometry of the inlet and outlet passage of the regenerative pump [17]. Maity et al. used CFD to study regenerative pumps. They found out that a curvature in the outlet flow domain increases the net pressure head by minimizing the vortex flow. Also the semicircular static fluid on the sides of the impeller enhances the circulatory fluid motion, thereby increasing the efficiency of the pump. Positioning of the blades on either side of the impeller by offsetting enhances the fluid motion and results in the net increase in static and net pressure head. The different number of impeller vanes on either side of impeller will also contribute to the increase in net pressure head [18].

In this paper, a numerical study has been carried out in order to investigate the effect of blade angle on the performance of a regenerative pump. Also an analysis of flow pattern in regenerative pump at different flow coefficients was done. The objective of this work is to improve the performance of regenerative pumps by modifications of blades geometry. Two types of impeller were designed. The first one has symmetric angle blades and the second one with nonsymmetric angle blades. The blades inlet and outlet of the first group were designed in six different angles of ±10°, ±30°, and ±50°. For the second group the inlet angle was set to 0° and six different angles of ±10°, ±30°, and ±50° were designed for the outlet of the blades. The results of CFD were validated with experimental results of a regenerative pump. The results of numerical investigation are used to improve the performance of regenerative pump.

2. Experiments

2.1. Specifics of Regenerative Pump. Components of the regenerative pump are shown in Figure 1. Typically, a regenerative pump consists of an impeller with blades at its periphery, inlet port, discharge port, stripper to isolate the high-pressure discharge from the low-pressure inlet, flow passage, and a casing. The main geometric parameters of the tested regenerative pump are presented in Table 1 and Figure 2.

2.2. Experiments Apparatus and Procedure. Figure 3 shows the arrangement of test rig. A reservoir tank with the capacity of 200 liters was employed in order to store and ultimately receive water. A control valve was installed in the return line to the reservoir tank to adjust the flow rate. The flow rate was measured using a rotameter which was calibrated. Results of calibration test are presented in Table 2.

The pump was driven by a 500-watt induction motor operating at a constant speed of 2900 rpm. A watt meter is used to measure the power consumption of the electropump.

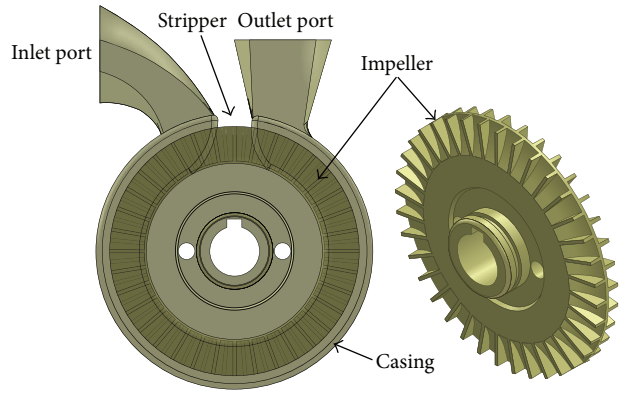

Figure 1: Schematic of the regenerative pump.

Table 1: Geometric specifications of regenerative pump.

Parameters	Unit	Value
Number of blades in each side, N	—	36
Tip radius of casing, r_S	(mm)	36
Tip radius of blade, r_T	(mm)	32.5
Hub radius of blade, r_H	(mm)	23.5
Height of blade, h	(mm)	9
Width of the blade, b	(mm)	3.1
Width of the channel, d	(mm)	4.3
Angle of stripper, θ_s	(°)	16
Blade angle, β	(°)	0, ±10, ±30, ±50

Table 2: Results of calibration test for rotameter.

Rotameter flow rate (lit/min)	Calibration (lit/min)	Correction coefficient
40	39.999	0.999
35	35.145	1.004
30	29.849	0.995
25	24.064	0.963
20	19.842	0.992
15	15.291	1.019
10	11.100	1.110

The performance curve of the electromotor is shown in Figure 4, which was obtained using a dynamometer, separately.

The angular speed was measured using a proximity sensor. The inlet and outlet pressures were measured using two analog pressure gauges.

The uncertainty in the measurement of flow rate was about ±3%. And the pressures were measured with the uncertainty of ±1%.

3. Numerical Simulation and Model Description

The commercial software CFX-13 was used to solve the full three-dimensional Reynolds-averaged Navier-Stokes equations in this numerical study. The basic tool required for the

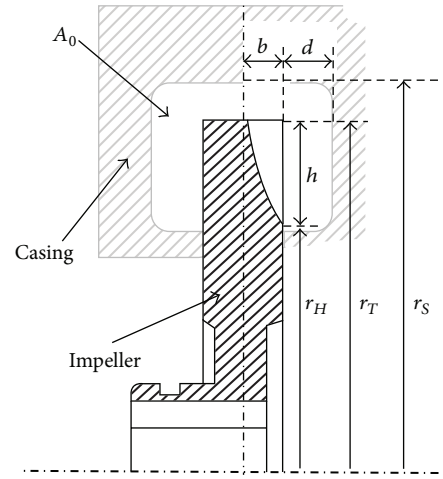

Figure 2: Regenerative pump geometric parameters.

derivation of the RANS equations from the instantaneous Navier-Stokes equations is the Reynolds decomposition. Reynolds decomposition refers to separation of the flow variable (like velocity u) into the mean (time-averaged) component ($\overline{u}$) and the fluctuating component (u'). The Navier-Stokes equations of motion for an incompressible Newtonian fluid, expressed in tensor notation, are as follows:

$$\frac{\partial \overline{u}_i}{\partial x_i} = 0,$$
$$\frac{\partial \overline{u}_i}{\partial t} + \overline{u}_j \frac{\partial \overline{u}_i}{\partial x_j} + \overline{u'_j \frac{\partial u'_i}{\partial x_j}} = \overline{f}_i - \frac{1}{\rho}\frac{\partial \overline{p}}{\partial x_i} + \nu \frac{\partial^2 \overline{u}_i}{\partial x_j \partial x_i}, \quad (1)$$

where f_i is a vector, representing external forces. Using the equation of conservation of mass, with slight variations, momentum equation becomes as follows:

$$\rho \frac{\partial \overline{u}_i}{\partial t} + \rho \overline{u}_j \frac{\partial \overline{u}_i}{\partial x_j} = \rho \overline{f}_i + \frac{\partial}{\partial x_i}\left[-\overline{p}\delta_{ij} + 2\mu \overline{S}_{ij} - \rho \overline{u'_i u'_j}\right], \quad (2)$$

where $\overline{S}_{ij} = (1/2)(\partial \overline{u}_i/\partial x_j + \partial \overline{u}_j/\partial x_i)$ is the mean rate of strain tensor. Finally, since integration in time removes the time dependence of the resultant terms, the time derivative must be eliminated, leaving

$$\rho \overline{u}_j \frac{\partial \overline{u}_i}{\partial x_j} = \rho \overline{f}_i + \frac{\partial}{\partial x_i}\left[-\overline{p}\delta_{ij} + 2\mu \overline{S}_{ij} - \rho \overline{u'_i u'_j}\right]. \quad (3)$$

The solver was a 3D CFD code. The governing equations are discretized using the finite element finite volume method in this code. To achieve high accuracy, the high resolution scheme was applied for discretization of momentum equation, pressure, turbulent kinetic energy, and turbulent dissipation rate.

For grid generation, the computing space is divided into two parts consisting of flow channel and impeller. The 3D models of them were generated and meshed separately. Since generating mesh for whole impeller causes a lack of precise

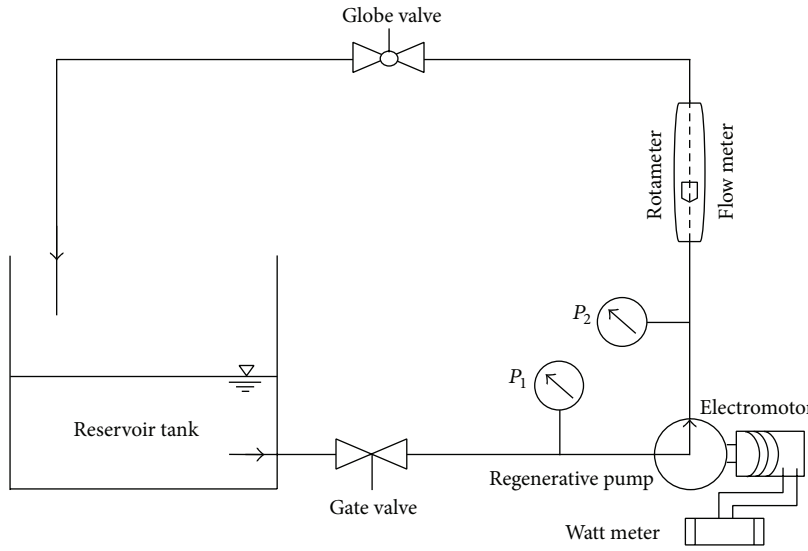

Figure 3: Schematic of regenerative pump test rig.

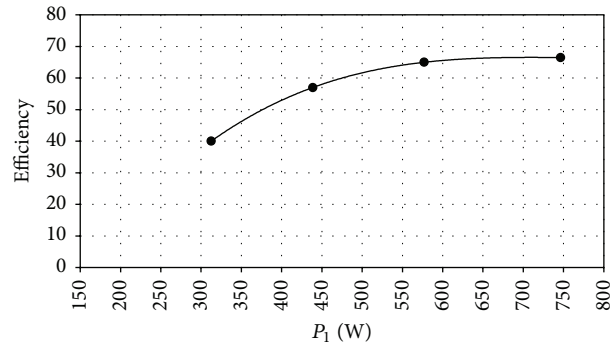

Figure 4: Performance curve of electromotor (efficiency versus power consumption).

control and prolongs the grid generation, one blade from each side of impeller was selected for grid generation. Finally this part was rotated 35 times to have a complete impeller. During mesh generation, orthogonal quality, skewness, and aspect ratio are assured to be in desirable range. Skewness was held below 0.9 and aspect ratios of greater than 5 : 1 were not applied. Hexahedral cells were used for important regions with curvature and strong gradients and tetrahedral cells for other regions. Figure 5 shows the generated grids for the blades and flow channel. Due to existence of intensive gradients in blades region and also complex spiral flow pattern in them, structured grids were used for the region between blades. Mesh clustering was applied for important regions such as interface between flow channel and impeller. Excessive expansion of cells in the direction normal to the walls was avoided. At least a few cells should be considered inside the boundary layer and for the pump this was kept to a minimum of 5 cells. Five layers were considered for the interface between impeller and flow channel.

For numerical simulation, the convergence criteria were set at maximum residuals of 1×10^{-4}. Water at 25°C was selected as the working fluid. A constant total pressure boundary condition was applied for inlet region of pump while a constant mass flow rate (normal to the boundary) was implemented for outlet region of flow channel.

The flow channel domain was stationary and the impeller domain was rotating at constant speed. For quasi-steady simulation, the grids between impeller and flow channel are connected by means of a frozen rotor interface. In the case of transient simulation, transient rotor stator was selected for connection between impeller and flow channel grids.

As shown in Figure 6, for grid independency studies, eight adapted grid sizes were assessed. It was found that, by increasing the number of cells from 2.52×10^6 to 3.35×10^6, changes in hydraulic efficiency are about 0.019% and further grid refinement from 3.35×10^6 cells to 3.86×10^6 cells decreases the hydraulic efficiency about 0.016%. So, grid independence was established at around 3.35×10^6 cells.

3.1. CFD Results Validation. For validation of CFD results, the performance curve of regenerative pump, obtained from numerical simulations, was compared with the experimental

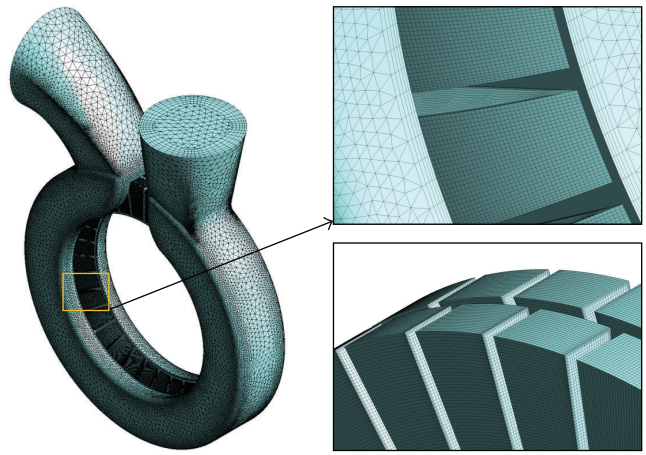

Figure 5: CFD grids of geometries.

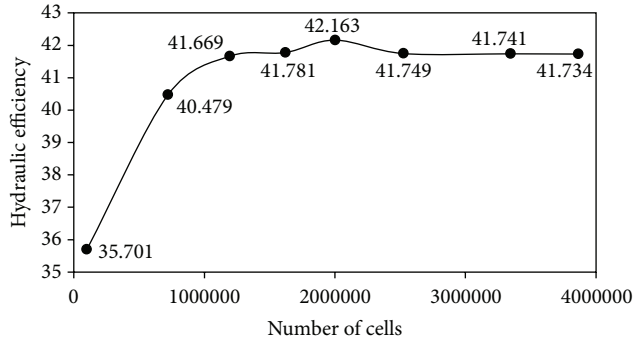

Figure 6: Hydraulic efficiency versus number of cells.

data. In this study, three well-known turbulence models (standard k-ε, low-Reynolds k-ω, and SST) were examined. Standard k-ε is a high-Re turbulence model that is able to predict inviscid flow regime properly. So, this model needs wall function approximation to solve viscous region near walls. The low-Re k-ω turbulence model could be used for entire flow region even near walls. The low-Re k-ω model would typically require a near wall resolution of $y^+ < 2$. In turbomachinery flows, even $y^+ < 2$ cannot be guaranteed and for this reason, a new near wall treatment was developed for the k-ω models. It allows for smooth shift from k-ω model to a wall function formulation regarding local y^+ value [19]. The SST turbulence model combines the k-ω turbulence model and k-ε turbulence model such that k-ω is used in the inner region of the boundary layer and switches to k-ε in the free shear flow.

Since the regenerative pump complies with the same affinity laws as centrifugal and axial pumps, the performance curves are presented using dimensionless flow coefficient (ϕ), head coefficient (ψ), and efficiency (η) which is defined as the ratio between the hydraulic power transferred to the working fluid and the mechanical power (P) introduced into the system by the impeller. Pump characteristic flow, head, power, and efficiency coefficients can be expressed in conventional dimensionless terms (4)–(7) [6]:

$$\psi = \frac{gH}{U_g^2}, \tag{4}$$

$$\phi = \frac{Q}{A_o U_g}, \tag{5}$$

$$\tau = \frac{P}{\rho A_o U_g^3}, \tag{6}$$

$$\eta = \frac{\rho Q g H}{P} = \frac{\phi\psi}{\tau}. \tag{7}$$

The performance curves of numerical simulations, obtained from three turbulence models, are compared with the experimental data in Figure 7.

As it can be seen in Figure 7(a), the k-ω turbulence model has better agreement with experimental data than k-ε and SST turbulence models. However, because of very complex flow in regenerative pump at low flow coefficients, the level of agreement with the measured data is not as close as those for higher flow coefficients. Although all three turbulence

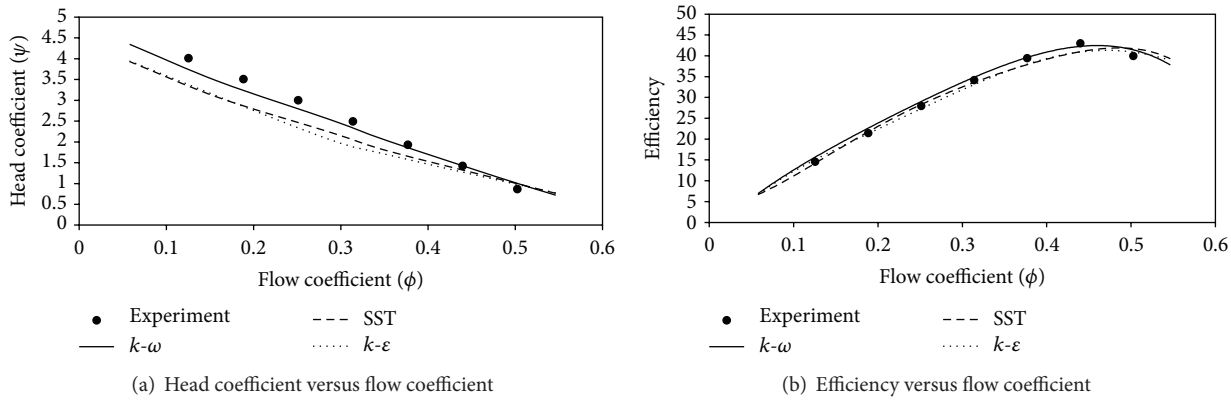

(a) Head coefficient versus flow coefficient

(b) Efficiency versus flow coefficient

Figure 7: Comparison of regenerative pump performance curves obtained from numerical simulations with experimental data.

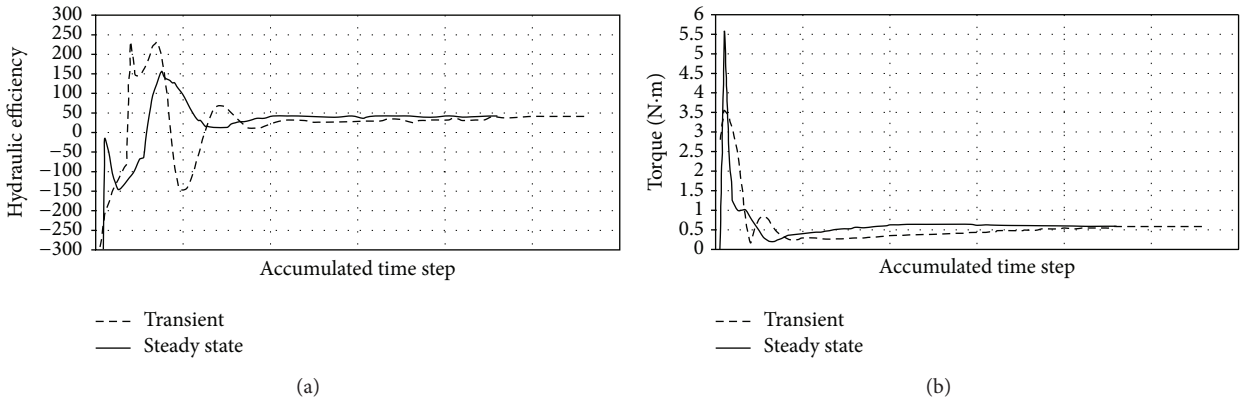

(a)

(b)

Figure 8: Variations in hydraulic efficiency of the pump and torque on impeller during accumulated time steps.

models have good trends in high flow coefficients, results of CFD simulations showed that, unlike k-ω turbulence model, the k-ε and SST turbulence models were not acceptable for prediction of the performance of regenerative pumps at lower flow coefficients. So, the k-ω turbulence model with automatic near wall treatments was carried out for numerical study. The low-Reynolds k-ω turbulence model is developed by Wilcox [20]. The kinematic eddy viscosity is obtained from the following equation:

$$\upsilon_t = \frac{k}{\omega}. \tag{8}$$

The evolution of k and ω is modelled with two transport equations:

$$\frac{\partial}{\partial x_j}\left(U_j k\right) = \frac{\partial}{\partial x_j}\left[\left(\nu + \frac{\nu_t}{\sigma_k}\right)\frac{\partial k}{\partial x_j}\right] + P_k - \beta' k\omega, \tag{9}$$

$$\frac{\partial}{\partial x_j}\left(U_j \omega\right) = \frac{\partial}{\partial x_j}\left[\left(\nu + \frac{\nu_t}{\sigma_\omega}\right)\frac{\partial \omega}{\partial x_j}\right] + \alpha\frac{\omega}{k}P_k - \beta\omega^2, \tag{10}$$

where constants β, β', σ_k, σ_ω, and α are presented in Table 3.

Table 3: Constants for the low-Reynolds k-ω turbulence model.

β	β'	σ_k	σ_ω	α
3/40	0.09	2	2.0	5/9

4. Results

4.1. Analysis of Flow Pattern in Regenerative Pump. According to results of other researchers, steady-state approximation for numerical simulations of regenerative pumps would represent good results [15, 16]. But since the nature of the flow in regenerative pump is unsteady, a transient simulation was accomplished just for main geometry of the pump to evaluate the results of quasi-steady simulations. The time step selected to update the relative position between impeller and casing is $5.68e-05$. This time step provides 1° rotation of the rotor between iterations, at rotational speed of 2900 rpm. The numerical solutions were carried out until the transient fluctuations of the flow variables became periodic. About three complete rotations of impeller are required to achieve convergence. Figures 8(a) and 8(b) show the variations in hydraulic

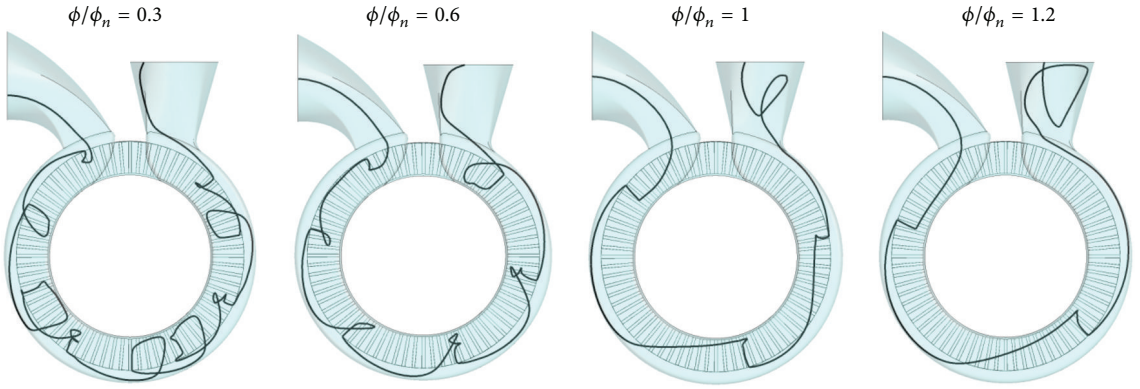

Figure 9: Fluid particle path lines at four different flow coefficients.

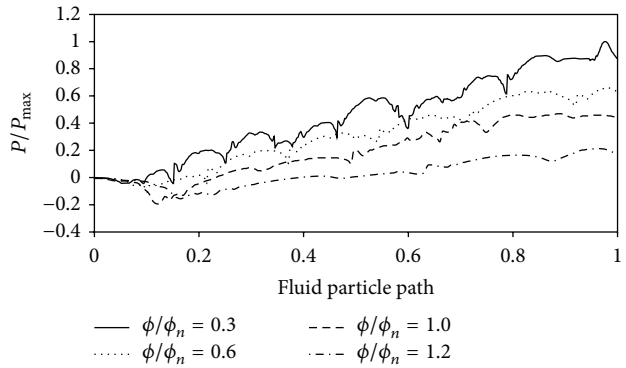

Figure 10: Comparison of pressure variation along a particle path line for four flow coefficients.

efficiency of the pump and torque on impeller during accumulated time steps for steady and transient numerical simulations at design point. As it can be seen, the difference between the final results is not considerable. The difference between the hydraulic efficiencies and torques, obtained from these two methods, is about 2.6% and 1.7%, respectively. So the results obtained from quasi-steady simulations would be reliable. Since the unsteady simulations are time-consuming and due to high number of simulations in this study, the flow in regenerative pump was assumed steady state and validated with experimental results as mentioned before.

Figure 9 shows the fluid particle path line in regenerative pump for four flow coefficients. As it can be seen the number of rotations of fluid increases by reduction in flow coefficient. Pressure variation along a streamline at design point (ϕ_n) and three other flow coefficients is shown in Figure 10.

As it can be seen in Figure 10, there are some fluctuations in the curves that increase with reduction in flow coefficient. The number of fluctuations in these curves indicates the number of rotations of fluid in regenerative pump. The minimum points in fluctuations of the curves in Figure 10 are related to entry of blades and the maximum ones are related to exit of blades. The head of pump decreases during passing through the channel of the pump because of rotational losses. It can be seen that, by reducing flow coefficient, while increasing the number of fluid rotations (Figure 9) in the pump, the head of pump increases. The growth in pressure by reduction of flow coefficient is also shown in pressure contours of Figure 11. The gradual growth in pressure is clearly obvious in these pressure contours (Figure 11).

The space between inlet and outlet regions of casing is occupied with stripper to separate low-pressure inlet from high-pressure outlet. The stripper helps the fluid to go out from discharge port. But, despite the existence of stripper, the amount of high-pressure fluid, trapped between blades, collides with the low-pressure fluid at inlet region of pump. So there is a loss at the inlet port of regenerative pump. As can be seen in Figure 10 there is a pressure drop at the beginning of the curves.

Figure 12 indicates the velocity distribution along the fluid particle path for different flow coefficients.

The amplitude of fluctuations of velocity curves reduces by reduction in flow coefficient. Figure 13 shows the velocity contours at design flow coefficient. The vortex at the inlet region, because of mixture of high-pressure outlet with low-pressure inlet, is obvious in Figure 13.

Two groups of impellers were employed in this study to investigate the effects of blade geometry modifications on the performance of a regenerative pump. The first type has symmetric angle blades and the second group nonsymmetric

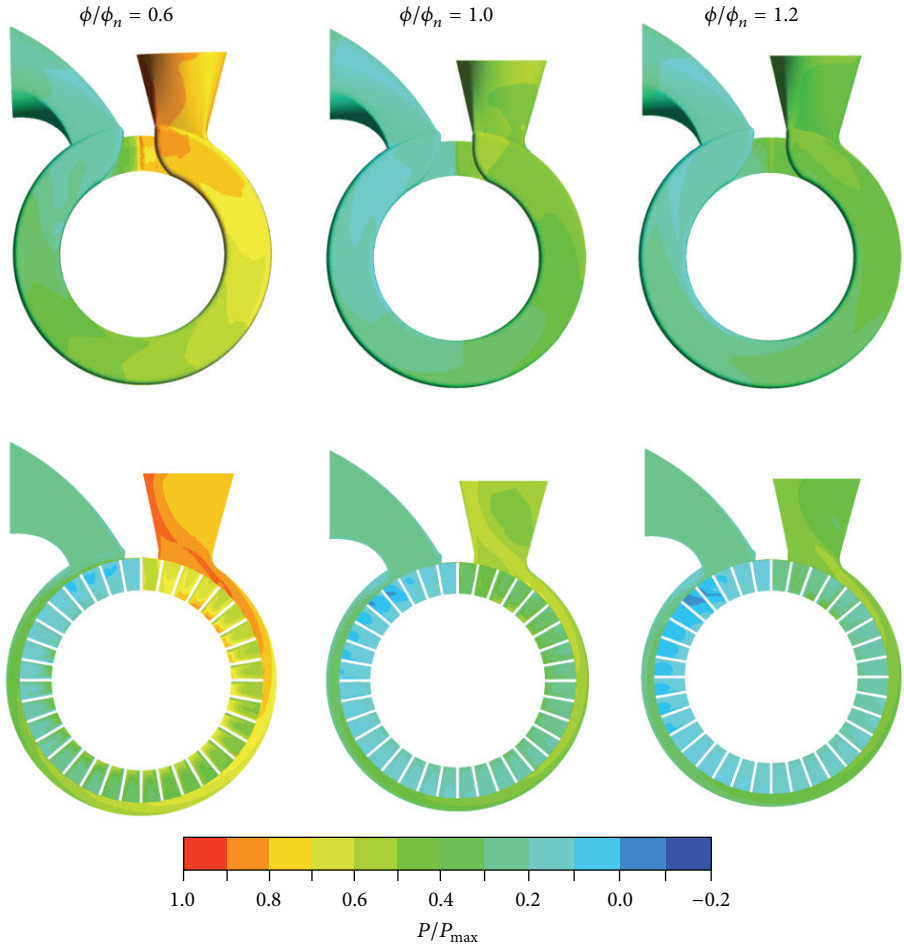

Figure 11: Pressure contours at $\phi/\phi_n = 0.6$, $\phi/\phi_n = 1$, and $\phi/\phi_n = 1.2$.

Table 4: Definition of symmetric and nonsymmetric angle blades.

(1) Symmetric angle blades	$\beta_1 = \beta_2 = \beta = \pm 10, \pm 30, \pm 50$
(2) Nonsymmetric angle blades	$\beta_1 = 0$, and $\beta_2 = \pm 10, \pm 30, \pm 50$

angle blades. The results obtained for these two groups of blades are presented and discussed.

4.2. Effect of Blade Geometry Modification. As presented in Table 4 and shown in Figure 14 the first group is named symmetric angle blades which have identical inlet/outlet angle. And the second group is nonsymmetric angle blades. In this group the inlet angle is constant and set to 0°.

A total of 12 impellers, as well as primary radial blades impeller, consist of symmetric forward blades ($\beta_1 = \beta_2 = +10°, +30°, +50°$), symmetric backward blades ($\beta_1 = \beta_2 = -10°, -30°, -50°$), nonsymmetric forward blades ($\beta_2 = +10°, +30°, +50°$), and nonsymmetric backward blades ($\beta_2 = -10°, -30°, -50°$) which were investigated in this numerical study.

The blade angle β is defined as shown in Figure 14. The positive sign of β represents the forward blade and the negative sign indicates backward blade. The 3D geometries and schematics of impellers are shown in Figure 15.

As mentioned before, the regenerative pumps have conformance with the affinity laws. So the flow coefficient (ϕ) and the head coefficient (ψ) and also hydraulic efficiency (η) defined by (4), (5), and (7) were applied for presenting the characteristic curves of the pump.

Figure 16 shows the performance curves, ψ versus ϕ for radial blade, forward and backward symmetric angle blade, and also forward and backward nonsymmetric angle blade impellers.

As it can be seen, in the case of symmetric angle with backward blades, the heads of pump are lower than those of radial blades impeller. But the condition for the case of symmetric angle with forward blades is different. It is observed that the head coefficients are increased at blades angle of +10° and +30° and reduced at angle of +50°. So there is an optimum angle in this range. Generally, it is obvious that increasing β, or, in other words, forwarding blades in centrifugal turbomachines, augments the Eulerian head. But in

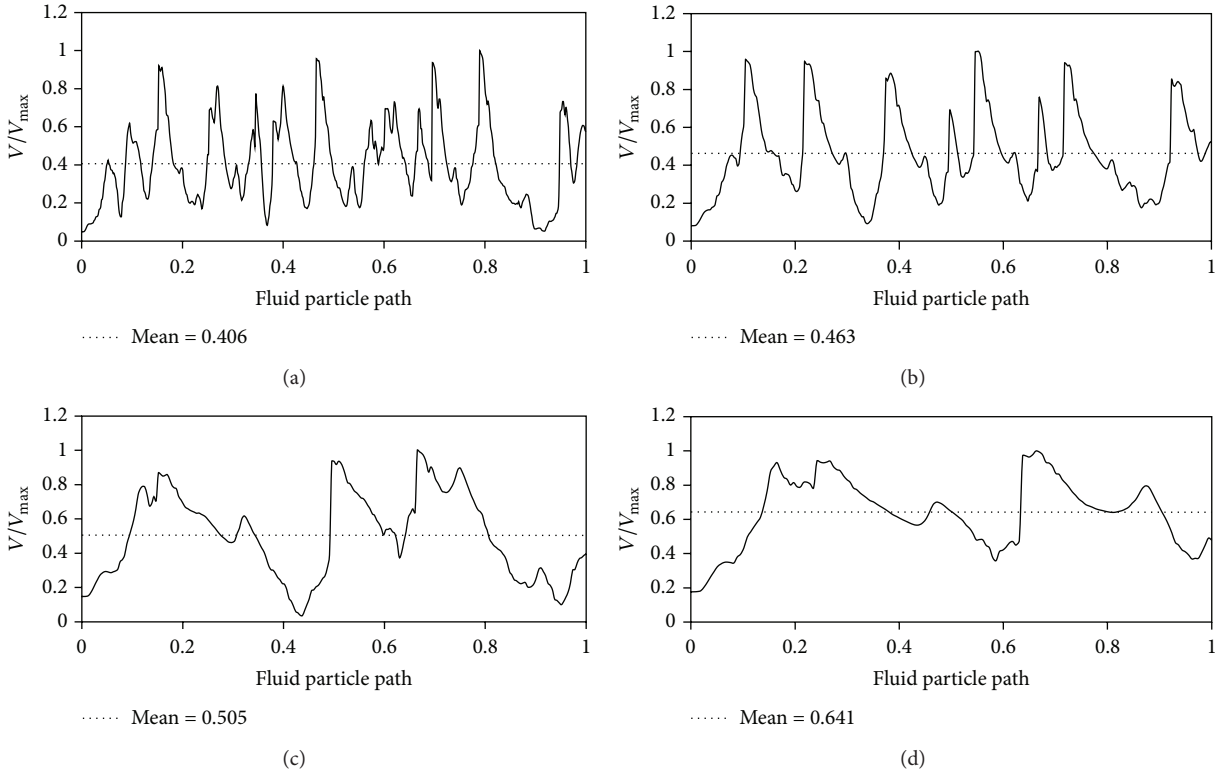

Figure 12: Velocity distribution along fluid particle path. (a) $\phi/\phi_n = 0.3$, (b) $\phi/\phi_n = 0.6$, (c) $\phi/\phi_n = 1.0$, and (d) $\phi/\phi_n = 1.2$.

regenerative pumps, the number of crock-screw circulations between blades and channel is an important parameter which can affect the total head. By increasing β, the number of crock-screw rotations will decrease because of the faster movement of fluid in the side channel. So, the outcome of these two parameters will affect the final total head.

It can be seen in Figure 16(b) that, in both cases of second group blades, the head coefficients are reduced by increasing the absolute value of β. However, at angles of $\beta_2 = \pm 10^\circ$, for flow coefficients higher than 0.35, it is observed that there are not any considerable differences relative to those of radial blades in the head coefficients. Both cases of nonsymmetric angle blades have not better performance than radial blades impeller. But it is obvious that the performance of backward blades is better than forward ones at lower flow coefficients. At shut-off condition ($\phi = 0$), the head coefficient of nonsymmetric angle forward blade with $\beta_2 = +30^\circ$ is about 2.75 while at the same condition the head coefficient for backward blade with $\beta_2 = -30^\circ$ is about 3.25. Also for $\beta_2 = +50^\circ$ and $\beta_2 = -50^\circ$ the head coefficients are, respectively, equal to 1.8 and 2.25 at shut-off condition.

The comparison of efficiency curves is shown in Figure 17. It is worth noting that the best efficiency point of the regenerative pump with radial blades impeller is found at $\phi_n = 0.47$ with about 42.5%. As it can be seen in Figure 17(a), there is not any considerable change in efficiency at $\phi < 0.35$ for the case of forward blades. It is observed that, at design flow coefficient ($\phi_n = 0.47$), the maximum efficiency of the 10° forward blades is about 44.7% which is about 2.2% higher than that of radial blades. The maximum efficiency for the case of 30° forward blades is about 1% higher than best efficiency of radial blades. But by increasing β to 50°, the maximum efficiency is decreased about 3%. In the case of backward blades, at angle of -10°, there is not significant change in efficiency curves relative to radial blades. But it seems that, in the range of $0.3 < \phi < 0.45$, the radial blades have better efficiency. With decreasing β, the efficiency curves decline except at very low flow coefficients. A significant falling is observed at angle of -50°. And it was seen that the best efficiency point is changed at angle of -50°.

For nonsymmetric angle blades, as it can be seen in Figure 17(b), at angle of $+10^\circ$ forward case, there is not any significant change in efficiency curve relative to that of radial blades in whole range of flow coefficients. It was found that the more the blades angle β increases the more the efficiencies decrease. The same conditions occur for nonsymmetric backward blades. The efficiency curve at angle of -10° is almost coincident on that of radial blades. By decreasing β to -30° the efficiency decreases in whole range of flow rates. The same as symmetric angle backward blades, the best efficiency point is shifted to lower flow coefficient at angle of -50° and also a significant falling is observed.

For better comparison between these types of blades and effect of changing angles on the performance of regenerative pump, Figure 18 is drawn.

It is obvious from Figure 18 that symmetric angle with forward blades has better performance than nonsymmetric angle blades. It is observed that the performance of both

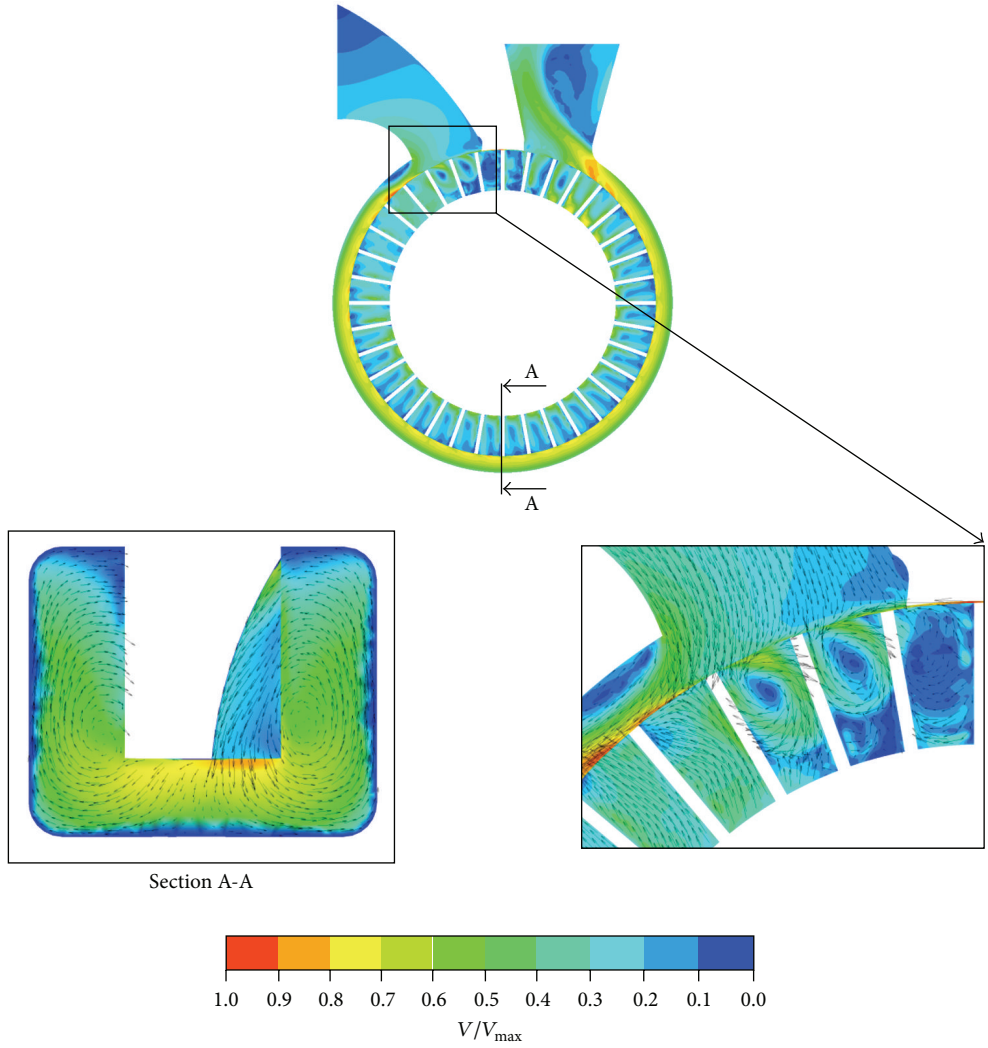

FIGURE 13: Velocity contour at design flow coefficient.

symmetric and nonsymmetric angle with backward blades is the same at $\phi/\phi_n = 0.7$ and $\phi/\phi_n = 1$, but at $\phi/\phi_n = 1.2$, nonsymmetric angle blades have higher head coefficients. Also it should be noted that the highest head coefficient occurs at angle $+10 < \beta < +30$ of symmetric angle blades. So, there is an optimum angle in this range of β. Figure 19 is drawn to compare the effect of the blades angle on efficiency at design flow coefficient. As it is observed, symmetric angle blades have better efficiency than radial blades at angles of $\pm 10^\circ$ and $+30^\circ$ or in other words the curve exhibits that, for $-10 < \beta < +40$, the symmetric angle blades have higher efficiency relative to radial blades. In the case of nonsymmetric angle blades, it was found that only the blades angle between 0 and about 10° has better efficiency than radial blades. But a significant improvement is not observed.

Results at design flow coefficient for all blades are presented in Table 5.

Generally, it was found out from curves of Figures 18 and 19 that regenerative pumps with symmetric angle forward blades have better performance than other types. As can be seen in Figure 20, a polynomial curve was fitted to the data obtained from numerical simulations to find the angle which has the best efficiency. The maximum efficiency takes place at angle of $+15.5^\circ$ as shown in Figure 20.

5. Conclusions

In this study, a numerical investigation has been carried out in order to study the effect of blade angle on the performance of a regenerative pump. A total of 12 impellers, as well as primary radial blades impeller, consist of symmetric forward and backward blades ($\beta_1 = \beta_2 = \beta = \pm 10^\circ, \pm 30^\circ, \pm 50^\circ$), nonsymmetric forward and backward blades ($\beta_2 = \pm 10^\circ, \pm 30^\circ, \pm 50^\circ$), which were investigated in this numerical study. The results showed that, in the case of symmetric angle with backward blades, the head coefficients of the pump are lower than those of radial blades impeller. It is observed in the case of symmetric angle with forward blades that the head

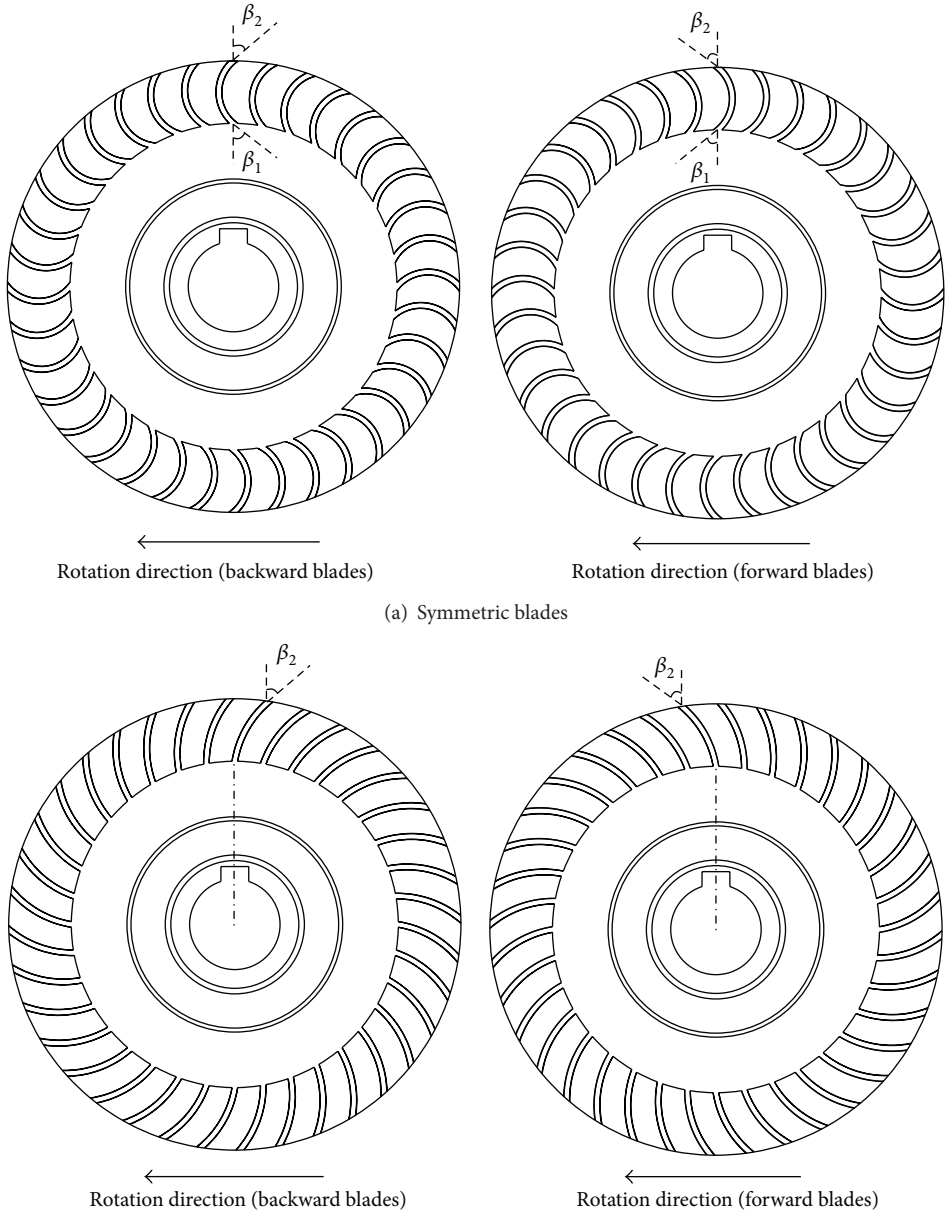

Figure 14: Schematic of blades: (a) symmetric blades and (b) nonsymmetric blades.

coefficients are increased at blades angle of +10° and +30° and reduced at angle of +50° relative to radial blades. Both cases (backward/forward) of nonsymmetric angle blades have not better performance than radial blades impeller. Results showed that, for symmetric angle blades, there are not any significant changes in efficiency at $\phi < 0.35$ for the case of forward blades. Also the maximum efficiency of the 10° symmetric angle forward blades is about 44.7% which is about 2.2% higher than that of radial blades. In the case of symmetric angle backward blades, with decreasing β, the efficiency curves decline except at very low flow coefficients. For nonsymmetric angle blades, at angles of ±10°, there are not any significant changes in efficiency curves relative to that of radial blades, in whole range of flow coefficients. Generally, it was found that regenerative pumps with symmetric angle forward blades have better performance than other types. Also it should be noted that the highest head coefficient occurs at angle $+10 < \beta < +30$ of symmetric angle blades. To obtain the angle which has the best efficiency, a polynomial curve was fitted to the data obtained from numerical simulations for symmetric angle forward blades. It was found that the maximum efficiency occurs at angle of +15.5°.

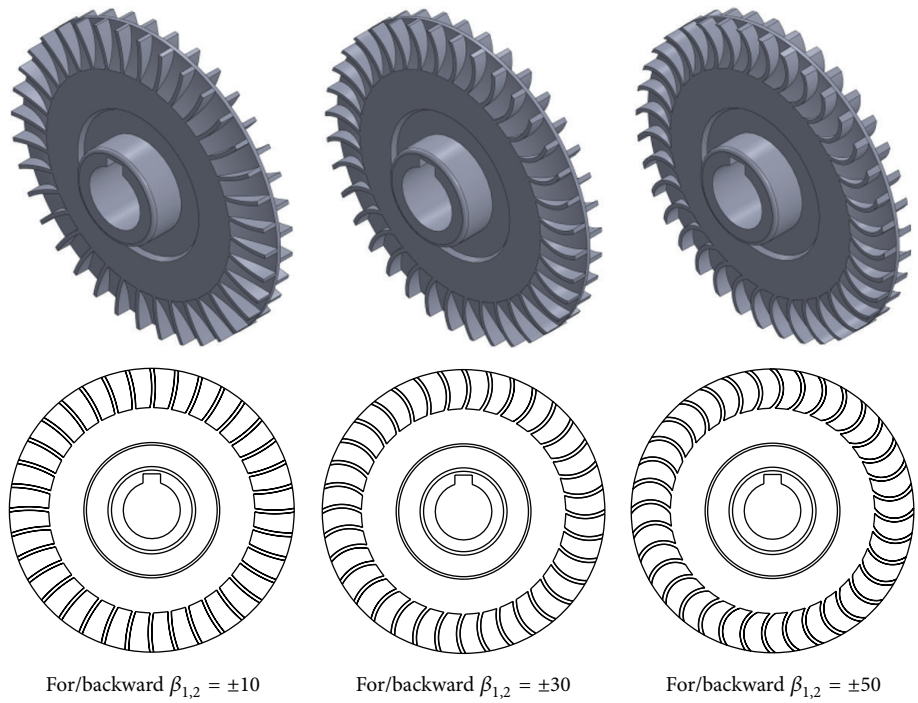

(a) Symmetric blades

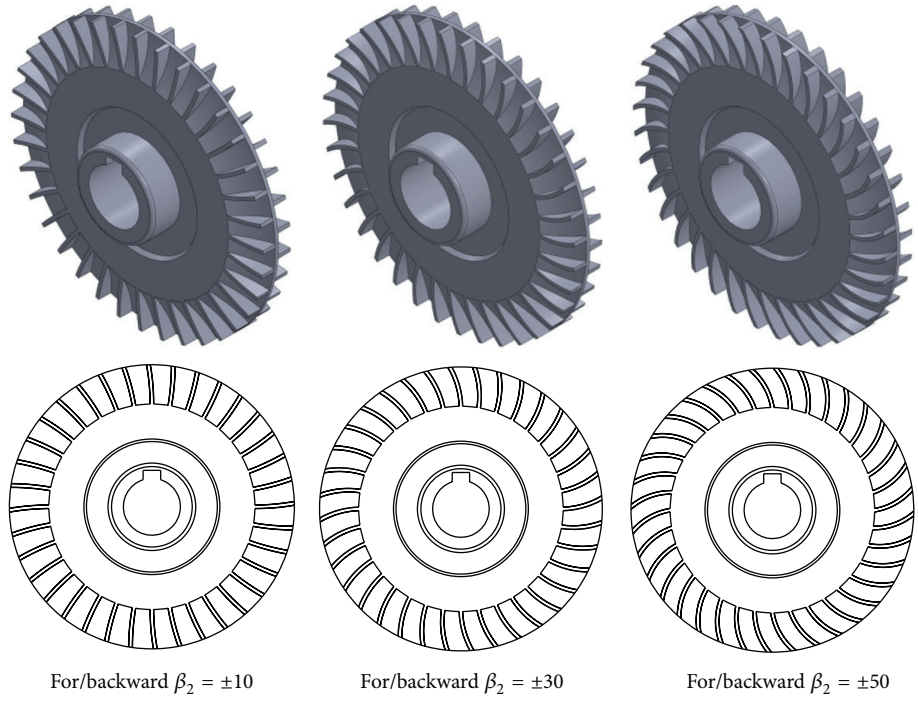

(b) Nonsymmetric blades ($\beta_1 = 0^\circ$)

FIGURE 15: Geometry of impellers: (a) symmetric blades and (b) nonsymmetric blades.

Nomenclatures

A_0: Cross section area (m^2)
b: Width of blade (mm)
d: Width of channel (mm)
f_i: External forces (N)
g: Gravity (ms^{-2})
H: Pump head (m)
h: Height of blade (mm)
k: Turbulence kinetic energy (m^2s^{-2})
N: Number of blades

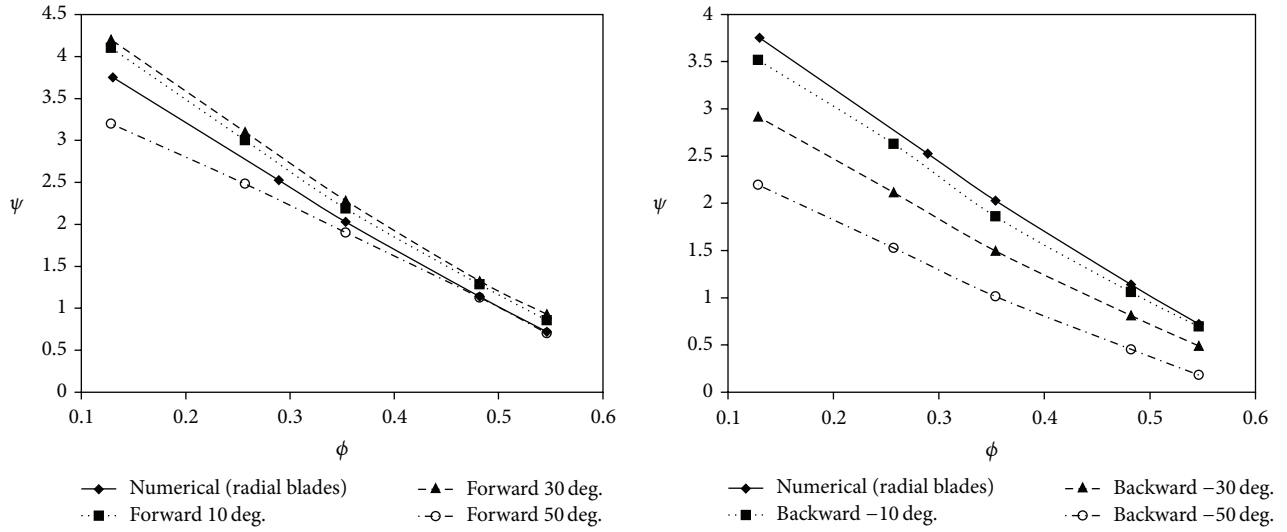

(a) Symmetric angle blades

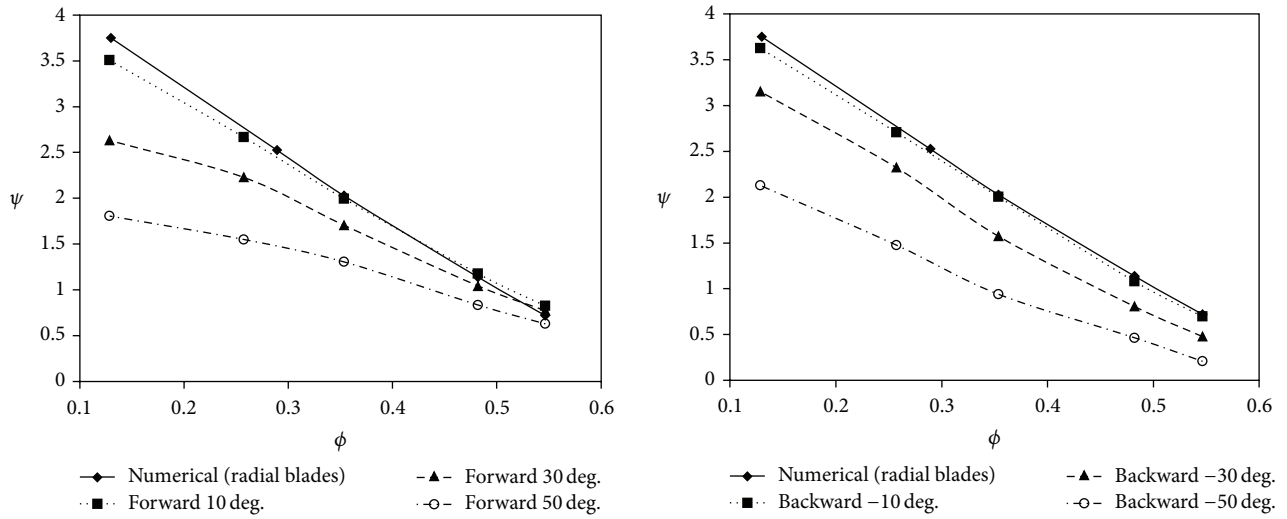

(b) Nonsymmetric angle blades

Figure 16: Characteristics curves of the regenerative pump: (a) symmetric blades and (b) nonsymmetric blades.

Table 5: Results of numerical study at design flow coefficient.

	Angles	Efficiency	Ψ (head coefficient)
Symmetric angle blades	$\beta_1 = \beta_2 = -50$	29.97	0.412
	$\beta_1 = \beta_2 = -30$	39.95	0.737
	$\beta_1 = \beta_2 = -10$	42.52	0.963
	$\beta_1 = \beta_2 = 0$	42.42	1.035
	$\beta_1 = \beta_2 = +10$	44.70	1.160
	$\beta_1 = \beta_2 = +30$	43.66	1.203
	$\beta_1 = \beta_2 = +50$	41.01	1.044
Nonsymmetric angle blades ($\beta_1 = 0$)	$\beta_2 = -50$	33.07	0.422
	$\beta_2 = -30$	39.10	0.733
	$\beta_2 = -10$	41.97	0.981
	$\beta_2 = 0$	42.42	1.035
	$\beta_2 = +10$	42.95	1.069
	$\beta_2 = +30$	40.71	0.947
	$\beta_2 = +50$	37.96	0.759

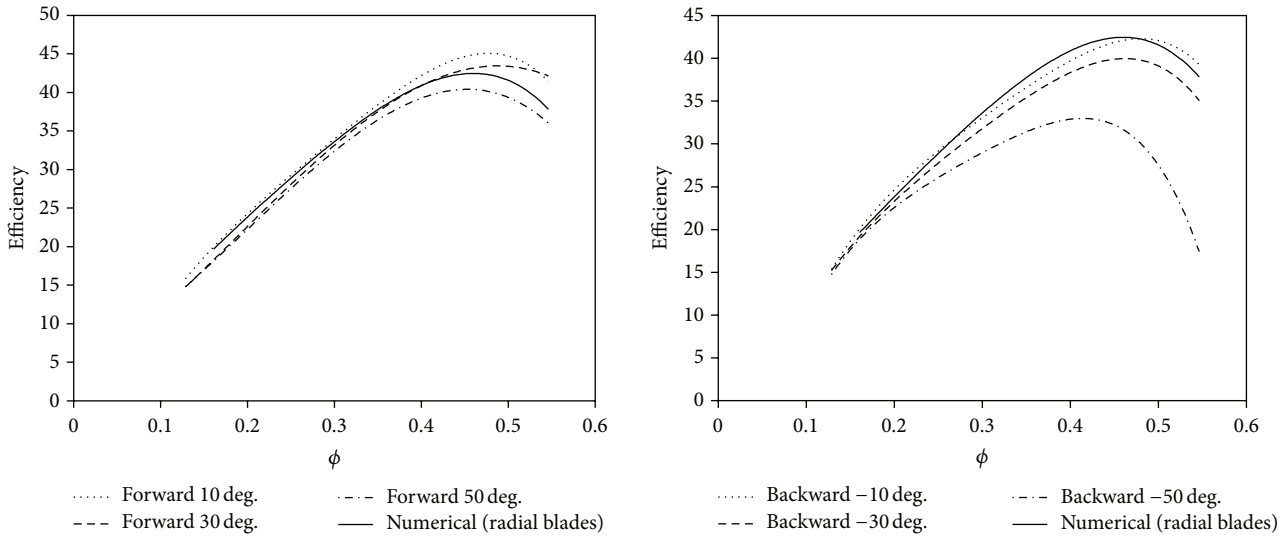

(a) Symmetric angle blades

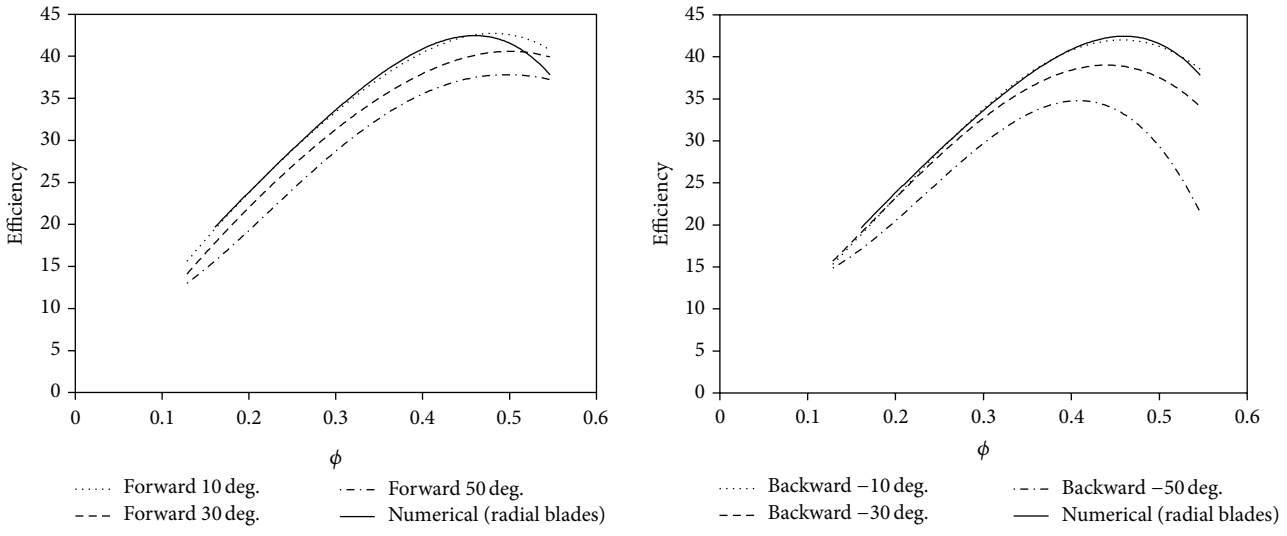

(b) Nonsymmetric angle blades

Figure 17: Efficiency curves of the regenerative pump: (a) symmetric blades and (b) nonsymmetric blades.

P_1: Power consumption of electromotor (watt)
P_k: Production rate of the turbulent kinetic Energy (m^2s^{-3})
p: Pressure (Pa)
Q: Volume flow rate (m^3s^{-1})
r_s: Tip radius of casing (mm)
r_T: Tip radius of blade (mm)
r_H: Hub radius of blade (mm)
S_{ij}: Strain rate tensor
U_g: Tangential speed (ms^{-1})
U_j: $[U, V, \overline{W}]$, mean velocity vector in tensor notation (ms^{-1})
u_i: $[u, v, w]$, instantaneous velocity vector in tensor notation (ms^{-1})
$\overline{u}_i$: $[\overline{u}, \overline{v}, \overline{w}]$, mean velocity vector in tensor notation (ms^{-1})
u_i': $[u', v', w']$, fluctuating velocity vector in tensor notation (ms^{-1})
V: Velocity (ms^{-1})
$V_{\max}$: Maximum velocity (ms^{-1})
x_i: $[X, Y, Z]$, Cartesian coordinates in tensor notation (m)
y^+: $\text{Exp}[(u^+ - 5.5)/2.5]$ distance from the wall (nondimensional).

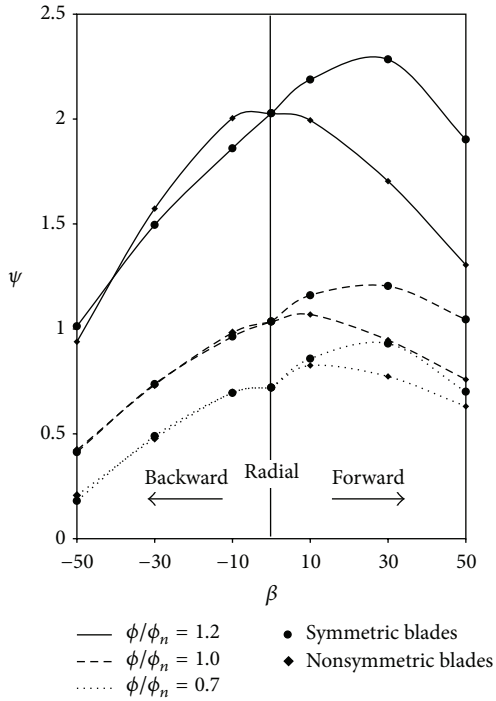

Figure 18: Comparison of head coefficients between all types of impellers with different blade angles at $\phi/\phi_n = 0.7$, $\phi/\phi_n = 1$, and $\phi/\phi_n = 1.2$.

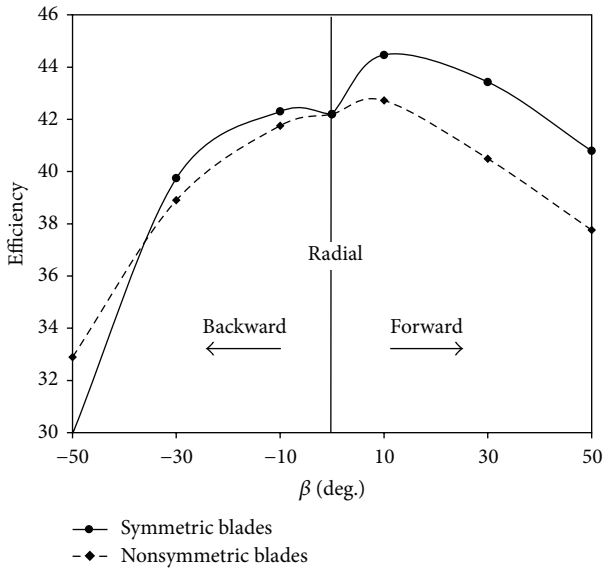

Figure 19: Comparison of efficiency between types of impeller at design flow coefficient.

Greek Symbols

$\alpha, \beta, \beta', \sigma_k, \sigma_\omega$: k-ω turbulence model coefficients
β: Blade angle (°)
ε: Dissipation rate (m^2s^{-3})
η: Hydraulic efficiency

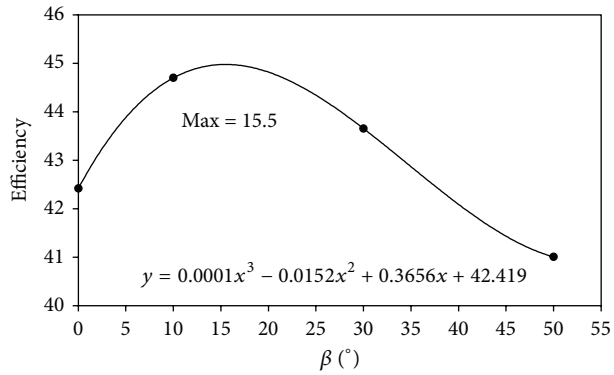

Figure 20: Curve fitting to the data of symmetric angle forward blades at design flow coefficient.

θ_s: Stripper angle (°)
ρ: Density (kgm^{-3})
υ: Kinematic viscosity (m^2s^{-1})
υ_t: Kinematic turbulent viscosity (m^2s^{-1})
μ: Dynamic viscosity ($kgm^{-1}s^{-1}$)
ϕ: Flow coefficient
ϕ_n: Flow coefficient at design point
ψ: Head coefficient
τ: Power coefficient
ω: Specific dissipation rate.

Conflict of Interests

The authors declare that there is no conflict of interests regarding the publication of this paper.

References

[1] I. S. Yoo, M. R. Park, and M. K. Chung, "Improved momentum exchange theory for incompressible regenerative turbomachines," *Proceedings of the Institution of Mechanical Engineers. Part A: Journal of Power and Energy*, vol. 219, no. 7, Article ID A09704, pp. 567–581, 2005.

[2] Y. Teshome and E. Dribsa, *CFD study of the performance of regenerative flow pump (RFP) with aerodynamic blade geometry [M.S. thesis]*, University of Addis Ababa, Addis Ababa, Ethiopia, 2007.

[3] W. A. Wilson, M. A. Santalo, and J. A. Oelrich, "A theory of the fluid dynamic mechanism of regenerative pumps," *Transactions of ASME*, vol. 77, pp. 1303–1316, 1955.

[4] J. W. Song, A. Engeda, and M. K. Chung, "A modified theory for the flow mechanism in a regenerative flow pump," *Proceedings of the Institution of Mechanical Engineers, Part A: Journal of Power and Energy*, vol. 217, no. 3, pp. 311–322, 2003.

[5] I. S. Yoo, M. R. Park, and M. K. Chung, "Hydraulic design of a regenerative flow pump for an artificial heart pump," *Proceedings of the Institution of Mechanical Engineers A Journal of Power and Energy*, vol. 220, no. 7, pp. 699–706, 2006.

[6] W. C. Choi, I. S. Yoo, M. R. Park, and M. K. Chung, "Experimental study on the effect of blade angle on regenerative pump performance," *Proceedings of the Institution of Mechanical*

Engineers Part A: Journal of Power and Energy, vol. 227, no. 5, pp. 585–592, 2013.

[7] M. Shimosaka and S. Yamazaki, "Research on the characteristics of regenerative pump : 1st report, influences of flow channel and impeller," *Bulletin of JSME*, vol. 3, no. 10, pp. 185–190, 1960.

[8] S. Yamazaki and Y. Tomita, "Research on the performance of the regenerative pump with non-radial vanes," *Bulletin of the JSME*, vol. 14, no. 77, pp. 1178–1186, 1971.

[9] S. Yamazaki, Y. Tomita, and T. Sasahara, "Research on the performance of the regenerative pump with nonradial vanes," *Bulletin of the JSME*, vol. 15, no. 81, pp. 337–343, 1972.

[10] Y. Tomita, S. Yamazaki, and T. Sasahara, "The scale effect and design method of the regenerative pump with nonradial vanes," *Bulletin of the JSME*, vol. 16, no. 98, pp. 1176–1183, 1973.

[11] G. Grabow, "Influence of the number of vanes and vane angle on the suction behaviour of regenerative pumps," in *Proceedings of the 5th Conference on Fluid Machinery*, vol. 1, pp. 351–364, Budapest, Hungry, September 1975.

[12] H. Sixsmith and H. Altmann, "A regenerative compressor," *Journal of Engineering for Industry*, vol. 99, no. 3, pp. 637–647, 1977.

[13] M. Badami, "Theoretical and experimental analysis of traditional and new periphery pumps," SAE Technical Paper Series 971074, 1997.

[14] T. Meakhail, O. P. Seung, D. A. Lee, and S. Mikhail, "A study of circulating flow in regenerative pump," in *Proceedings of the KSAS 1st International Session*, pp. 19–26, Gyeongju, Republic of Korea, 2003.

[15] F. Quail, T. Scanlon, and M. Stickland, "Design optimisation of a regenerative pump using numerical and experimental techniques," *International Journal of Numerical Methods for Heat & Fluid Flow*, vol. 21, no. 1, pp. 95–111, 2011.

[16] F. J. Quail, T. H. Scanlon, and A. Baumgartner, "Design study of a regenerative pump using one-dimensional and three-dimensional numerical techniques," *European Journal of Mechanics, B/Fluids*, vol. 31, no. 1, pp. 181–187, 2012.

[17] K. Vasudeva Karanth, M. S. Manjunath, S. Kumar, and N. Yagnesh Sharma, "Numerical study of a self priming regenerative pump for improved performance using geometric modifications," *International Journal of Current Engineering and Technology*, vol. 5, no. 1, pp. 104–109, 2015.

[18] A. Maity, V. Chandrashekharan, and M. W. Afzal, "Experimental and numerical investigation of regenerative centrifugal pump using CFD for performance enhancement," *International Journal of Current Engineering and Technology*, vol. 5, no. 4, pp. 2898–2903, 2015.

[19] H. Alemi, S. A. Nourbakhsh, M. Raisee, and A. F. Najafi, "Effects of volute curvature on performance of a low specific-speed centrifugal pump at design and off-design conditions," *Journal of Turbomachinery*, vol. 137, no. 4, pp. 041009-1–041009-10, 2015.

[20] D. C. Wilcox, "Multiscale model for turbulent flows," in *Proceedings of the AIAA 24th Aerospace Sciences Meeting*, AIAA Paper no. 86-0029, Reno, Nev, USA, January 1986.